

Determination of a Surrogate for Plutonium Electrorefining

Greg Chipman^{a,*}, Bryant Johnson^a, Suhee Choi^b, Chao Zhang^c, Michael Simpson^b, Devin Rappleye^a

^aDepartment of Chemical Engineering, Brigham Young University, Provo, UT 84602, USA

^bDepartment of Material Science and Engineering, University of Utah, Salt Lake City, UT 84112, USA

^cMaterial Science Division, Lawrence Livermore National Laboratory, Livermore, CA 94551-0808, USA

Abstract

Conducting research experiments on plutonium electrorefining is difficult due to the significant hazards and regulations associated with nuclear materials. Finding a surrogate for plutonium electrorefining studies would enable more fundamental research to be conducted. Potential surrogates were first identified by determining the physical properties required to conduct electrorefining at the same conditions commonly used in plutonium electrorefining, a molten metal and molten CaCl_2 at 1123 K. Ce-CeCl_3 , In-InCl_3 , and Pb-PbCl_2 were the only potential surrogates identified using these constraints. Sn-SnCl_2 was also tested at these same conditions. More potential surrogates were identified by changing the matrix salt and operating temperature. This expanded the potential surrogate list to also include Zn-ZnCl_2 , Sn-SnCl_2 , and Bi-BiCl_3 . Zn-ZnCl_2 was used with the LiCl-CaCl_2 (65:35 mol%) eutectic at 773 K. Sn-SnCl_2 and Bi-BiCl_3 were used with the LiCl-KCl-CaCl_2 (50.5:44.2:5.3 mol%) eutectic at 673-773 K. Ce electrorefining in molten CaCl_2 resulted in a difficult to separate colloid mixture of Ce , Ca and Cl . Electrorefining rates for In in molten CaCl_2 were too slow due to InCl_3 volatilizing out of the molten salt. Only trace amounts of SnCl_2 was retained in the CaCl_2 at 1123 K resulting in impractical electrorefining rates. Zn metal product was successfully collected in the LiCl-CaCl_2 eutectic molten salt, but the metal obtained did not coalesce into one piece. Sn and Bi were successfully electrorefined in the LiCl-KCl-CaCl_2 eutectic molten salt and coalesced into product rings with high yields and coulombic efficiencies. While a surrogate could not be identified using the same conditions as plutonium electrorefining, two possible surrogates, Sn-SnCl_2 and Bi-BiCl_3 , were found that could imitate the physical configuration (i.e., molten salt on top of molten metal) of plutonium electrorefining at a reduced temperature using the eutectic LiCl-KCl-CaCl_2 salt at 673-773 K in place of CaCl_2 at 1123 K.

1. Introduction

Initial research on plutonium electrorefining in the 1960s focused on the development and characterization of the process [1–4]. In 1981, after nearly two decades of experience, Mullins and Morgan reported that electrorefining operating conditions have been determined “to permit termination of the run at a convenient time” and that “the electrolyzing current has never been optimized” [4]. Because of the importance of non-proliferation and plutonium’s radiotoxicity, acquiring and handling significant amounts of plutonium requires substantial security,

Accepted manuscript of the journal article: Chipman, G., Johnson, B., Choi, S., Zhang, C., Simpson, M., & Rappleye, D. (2023). Determination of a surrogate for plutonium electrorefining. *Journal of Nuclear Materials*, 586, 154680. <https://doi.org/10.1016/j.jnucmat.2023.154680>

© 2023 CC-BY-NC-ND license. <https://creativecommons.org/licenses/by-nc-nd/4.0/>

infrastructure, training, and regulatory compliance [5,6]. In addition to the safety, security, and regulatory challenges of working with plutonium, the high cost of performing work with plutonium limits the number of experiments that can be conducted. Therefore, finding a surrogate for plutonium electrorefining is necessary to reduce operational complexity and costs for fundamental science and engineering studies. Enabling these studies would help to increase the understanding of the charge transfer, mass transport, and other mechanisms in electrorefining a dense molten metal in molten salts.

Plutonium electrorefining occurs in molten salt electrolytes, typically CaCl_2 or equimolar NaCl-KCl , above the melting point of plutonium (914 K) and the melting point of the salt system (1045 K for CaCl_2 and 934 K for equimolar NaCl-KCl) [1]. Due to the high density of plutonium, the molten salt electrolyte sits atop a molten anode and cathode deposit. Plutonium electrorefining occurs in concentric, cylindrical ceramic crucibles with an impure molten anode in the inner crucible and a pure molten cathode deposit in the outer annulus creating a ring of product, as illustrated in Figure 1.

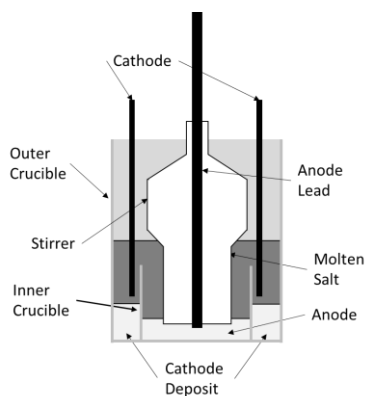


Figure 1: Illustration of a plutonium electrorefining set-up.

To simulate this mode of electrorefining, a surrogate metal needs to satisfy the following conditions at a minimum: (1) liquid at operating temperature, (2) denser than the molten salt, and (3) reduction potential within the electrochemical stability window of the molten salt.

If any one of these conditions is not met, surrogate electrorefining cannot be done in the same physical configuration as plutonium electrorefining. Floating or suspended metal deposits will cause shorting. The decomposition of the molten salt will prevent dissolution and deposition of the metal. Therefore, necessary properties to consider when selecting a surrogate for plutonium electrorefining include melting points, boiling points, liquid densities, and the standard reduction potentials of metal chlorides.

For initial surrogate identification, CaCl_2 was chosen as the molten salt electrolyte, which requires a sustained operating temperature near 1123 K. A plutonium electrorefining surrogate would ideally be a molten metal with a chloride that can be dissolved in molten CaCl_2 . Thus, a metal with a melting point less than 1123 K and boiling point greater than 1123 K is required. A density of the surrogate metal that is significantly greater than that of the molten CaCl_2 ($\sim 2000 \text{ kg m}^{-3}$ at 1123 K) is also needed to facilitate coalescence of the metal deposit.

Table 1 lists possible surrogate metals and their respective chlorides that meet all the minimum requirements to perform electrorefining in the same configuration as plutonium at 1123 K. Plutonium's properties are also included for reference. The standard reduction potential (E°) was estimated from the overall reaction for the redox couple, as shown below.



M is a place holder for the possible surrogate metals. The standard Gibb's free energy (ΔG°) of formation of M and Cl_2 is zero (i.e., assuming pure M and Cl_2). Hence, the negative value of ΔG° of formation of the metal chloride is the ΔG° of reduction relative to chlorine reduction reference potential. This is converted to potential by $E^\circ = -\Delta G^\circ/nF$. This approximated E° serves as an estimate for comparison.

As can be seen in Table 1, there are only a few potential surrogates that meet the minimum requirements at 1123 K. Ce appears to be the best suited surrogate based on the properties listed in Table 1. However, CeO_2 and Ce_2O_3 have a ΔG° of formation (per mole of O) that is less than the ΔG° of formation for PuO_2 , which may result in excessive oxide formation when molten Ce metal is in contact with ceramic crucibles [7]. $InCl_3$ has a boiling point less than 1123 K. However, it could be used if it can be captured in the matrix $CaCl_2$ salt, as has been done for $ZrCl_4$ in LiCl-KCl eutectic [8]. Lastly, $PbCl_2$ has a standard reduction potential significantly greater than $PuCl_3$.

While Ce's suitability would indicate that other lanthanide elements would be ideal surrogates for plutonium electrorefining, the high melting points of the other lanthanide elements (La = 1193 K, Pr = 1204 K, Nd = 1294 K, Gd = 1585 K) made it so that they would not be a molten metal at the typical operating temperature of plutonium electrorefining. Raising the temperature of operation to include other lanthanide metals was not considered due to furnace limitations and thermal limitations of stainless-steel parts (i.e., furnace well, liner, and electrode leads).

Table 1: Potential electrorefining surrogates that meet the minimum requirements to maintain the same electrorefining configuration as plutonium at 1123 K.

	Melting Point (K)	Boiling Point (K)	Density ($kg\ m^{-3}$)	E° (V vs Cl_2/Cl^-) ¹
Pu	913	3498	19,840	---
$PuCl_3$	1033	2040	---	-2.47
Ce	1071	3695	6,760	---
$CeCl_3$	1090	2000	---	-2.72
In	430	2343	7,310	---
$InCl_3$	856	1073	---	-1.44
Pb	600	2019	11,290	---
$PbCl_2$	774	1223	---	-1.08
¹ Calculated from data in Ref. [7]				

If a different matrix salt is used, the electrorefining operating temperature could be lowered. Ideally, this alternate matrix salt would still contain CaCl_2 to maintain some measure of chemical similarity to the targeted system. The eutectic salt system containing CaCl_2 identified in the open literature that offers the lowest melting point while maintaining the same electrochemical window is LiCl-KCl-CaCl_2 (50.5:44.2:5.3 mol%) with a liquidus temperature of 605 K [9]. Additionally, this molten salt has a lower density ($\sim 1700 \text{ kg m}^{-3}$ assuming ideal mixing) which may slightly extend the range of workable metal densities [10,11]. Changing the salt matrix expands the list of possible surrogates to also include the metal-metal chloride couples listed in Table 2.

Table 2: Potential electrorefining surrogates that meet the minimal requirements at a reduced operating temperature of 673 K.

	Melting Point (K)	Boiling Point (K)	Density (kg m^{-3})	E° (V vs Cl_2/Cl^-) ¹
Bi	545	1833	9,780	---
BiCl_3	500	720	---	-0.848
Sn	505	2543	7,310	---
SnCl_2	520	896	---	-1.242
Zn	693	1180	7,130	---
ZnCl_2	563	1005	---	-1.634
Tl	573	1730	11,710	---
TlCl	604	993	---	-1.657
¹ Calculated from data in Ref. [7]				

While the potential surrogates listed in Table 1 can more closely replicate plutonium electrorefining, the potential surrogates in Table 2 provide a few more options at the cost of changing the operating temperature and molten salt system. Both Pb and Tl were eliminated for consideration in this study due to their extreme toxicity, which is counterproductive to the aims of identifying a surrogate to simplify material handling and analysis.

Of all the surrogates identified, Ce is the only surrogate that has been investigated previously. Raraz focused on using Ce as a surrogate for plutonium electrorefining due to its similarity to plutonium, but an analysis of the electrorefining efficiency and yield was not possible due to side reactions and difficulties in separating Ce from the molten salt [12]. However, Ce was not eliminated from consideration because its near chemical similarity to plutonium warranted additional attempts to mitigate the issues identified by Raraz. Thus, the metal-metal chloride couples selected to investigate as surrogates are Ce- CeCl_3 , In- InCl_3 , Zn- ZnCl_2 , Sn- SnCl_2 , and Bi- BiCl_3 .

2. Material and Methods

The potential surrogates were investigated at three different locations: Brigham Young University-Provo (BYU), Ce- CeCl_3 and Bi- BiCl_3 ; University of Utah (UU), In- InCl_3 , Zn- ZnCl_2 , and small-scale Sn- SnCl_2 ; Lawrence Livermore National Laboratory (LLNL), large-scale Sn- SnCl_2 . Attempts were made to maintain consistency of methods across locations. However, there are some differences in methodology at each of the different locations, which are detailed in this section.

2.1. Cerium

For electrorefining, concentric and bonded yttria-stabilized MgO crucibles (Tateho Ozark Technical Ceramics, >98.5%), hereafter referred to as a MgO crucible for short, were used (see Figure 1. Ce ingots (99% REO, Alfa Aesar, 43977) were melted in the inner MgO crucible to form the anode. The outer MgO crucible contained CeCl₃ hydrate (99% REO, Alfa Aesar, 11325) mixed with CaCl₂ dihydrate (>99%, Alfa Aesar, 33296) after both salts were dried to serve as the electrolyte. The CeCl₃ hydrate was dried using a drying procedure from the literature [13]. The CaCl₂ dihydrate was dried by heating it in a drying oven (Across International, AT32e) under vacuum. The temperature of the oven was initially heated to 373 K for 8 hours, then heated to and held at 388 K for 8 hours. Lastly, the furnace was heated to and held at 522 K for 60 hours. After being dried in the drying oven, the CaCl₂ was heated to 1123 K for 4 hours then allowed to cool in the glovebox furnace well. Before melting, the dried CeCl₃ and CaCl₂ were added to the crucibles at a ratio to achieve 7.5 wt% CeCl₃ in CaCl₂. The same Ce ingots and salts were also used in the melt experiments. Yttria paint (Graphite Store, ARMC-634-YO) was applied to the inside of some Al₂O₃ crucibles (Advalue Tech, >99.6%, AL-2100) used for the Ce melt experiments to compare the reactivity of Ce in Al₂O₃ crucibles and Al₂O₃ crucibles coated with yttria paint.

2.2. Indium

CaCl₂ dihydrate was heated to 473 K overnight under vacuum to remove moisture. It was heated to 1123 K in the MgO crucible, after which anhydrous InCl₃ (99.99%, Alfa Aesar, 41977) was added to target 5 wt.%. In ingots (99.999%, Alfa Aesar, 14720) were melted in the inner MgO crucible to form the anode.

2.3. Zinc

CaCl₂ and LiCl (>99%, Sigma Aldrich, 310468) were mixed with a mole ratio of 65-35 mol% to form the eutectic molten salt for the experiment. Prior to mixing the salts, CaCl₂ dihydrate was dried by heating it in a quartz reactor under vacuum at 473 K overnight. Zn metal (99.9%, Alfa Aesar) was melted in the inner crucible to form the anode. Anhydrous ZnCl₂ (99.95%, Alfa Aesar, 87900) was added to the LiCl-CaCl₂ eutectic to achieve 5 wt.%. Then the mixture was melted in the MgO crucible.

2.4. Tin

For the small-scale experiments, anhydrous SnCl₂ (99.99%, Sigma Aldrich, 452335) was received as a powder and melted into larger pieces at 523 K for 1 hour in a glassy carbon crucible (SPI supplies). It was then ground into a coarse particulate. Dried CaCl₂ was heated to 1123 K in a MgO crucible. The SnCl₂ was added to the molten CaCl₂ to minimize potential loss due to evaporation during heat up. 5 wt.% SnCl₂ was the targeted electrolyte concentration.

For the large-scale experiments, the anode material was Sn ingots (99%, Thermo Scientific). SnCl₂ was added to the eutectic mixture of 50.5 mol% LiCl (99%, anhydrous, Thermo Scientific), 44.2 mol% KCl (99%, anhydrous, Thermo Scientific), and 5.3 mol% CaCl₂ (99%, Thermo Scientific, anhydrous, dried in house) eutectic. A concentration of 5 wt.% SnCl₂ was targeted.

2.5. Bismuth

Bi pieces (99.99% metals basis, Alfa Aesar, 12208) were melted in the inner crucible to act as the anode for electrorefining. Anhydrous BiCl_3 (99.9% metals basis, Alfa Aesar, 17115) was added to a eutectic mixture of 5.3 mol% CaCl_2 (dried as described in Section 2.1), 50.5 mol% LiCl (>99%, Alfa Aesar, 36217), and 44.2 mol% KCl (>99%, Alfa Aesar, 11595) after each was dried. BiCl_3 was mixed with LiCl-KCl-CaCl_2 eutectic to achieve a 13 wt.% BiCl_3 mixture before melting. The KCl and LiCl were dried using the vacuum drying oven. The KCl and LiCl were initially held under vacuum at room temperature for 8 hours, then heated to and held at 383 K for 8 hours. The oven was then heated to and held at 459 K for 8 hours. Lastly, the furnace was heated to and held at 522 K for 24 hours. Eutectic salt blocks were made using Al_2O_3 crucibles (Advalue Tech, >99.6%, AL-21000) by heating a eutectic salt mixture to 1023 K for 4 hours.

3. Experimental

All experiments were carried out in inert atmosphere gloveboxes, typically filled with argon gas (<10 ppm H_2O and O_2). The metal and salt were loaded into the crucibles. The loaded crucibles were placed in a stainless-steel container to protect the furnaces from overflow or leakage (e.g., cracked crucibles). The nested containers were placed in the furnace and heated to the operational temperature. Once the salt and metal were molten, the electrodes were lowered into the electrochemical cell. A motor was attached to the stir shaft, which doubled as the anode lead, to provide mixing of the cell. The stir shaft ran through the center of an alumina stirrer (AdValue Technology, >99.6% Al_2O_3). A power supply or potentiostat was connected to the electrode leads above the furnace to provide power to the cell.

The general setup of the electrorefining cell was a concentric crucible arrangement, as shown in Figure 1. The inner crucible being shorter than the outer crucible. In general, a two-electrode setup was used. The anode was the molten metal in the center crucible. The tungsten cathode (Midwest Tungsten Services, 99.95% W) consisted of a 1.27 mm thick, partial (340°) ring and was lowered into the annulus between the inner and outer crucible, as depicted in Figure 1. Table 3 lists the materials used and location for each of the experiments. Table 4 lists the amount of each material used, the operating temperature and duration of each run. In Table 3, the LiCl-CaCl_2 and LiCl-KCl-CaCl_2 represent the eutectic compositions of 65:35 mol% and 50.5:44.2:5.3 mol%, respectively. The amount of SnCl_2 entering the molten CaCl_2 is uncertain due to vaporization and other potential losses (e.g., hold-up, spillage). Hence, only the post-experiment total salt mass is reported in Table 4.

Table 3: Materials used for each experiment.

Run	Place	Metal	Metal Chloride	Base Salt	Crucible
Ce-1	BYU	Ce	N/A	CaCl ₂	Al ₂ O ₃
Ce-2	BYU	Ce	N/A	CaCl ₂	Y ₂ O ₃ coated Al ₂ O ₃
Ce-3	BYU	Ce	CeCl ₃	CaCl ₂	Y ₂ O ₃ stabilized MgO
Ce-4	BYU	Ce	CeCl ₃	CaCl ₂	Y ₂ O ₃ stabilized MgO
In-1	UU	In	InCl ₃	CaCl ₂	Y ₂ O ₃ stabilized MgO
Zn-1	UU	Zn	ZnCl ₂	LiCl-CaCl ₂	Y ₂ O ₃ stabilized MgO
Sn-1	UU	Sn	SnCl ₂	CaCl ₂	Y ₂ O ₃ stabilized MgO
Sn-2	UU	Sn	SnCl ₂	CaCl ₂	Y ₂ O ₃ stabilized MgO
Sn-3	UU	Sn	SnCl ₂	CaCl ₂	Y ₂ O ₃ stabilized MgO
Sn-4	UU	Sn	SnCl ₂	CaCl ₂	Y ₂ O ₃ stabilized MgO
Sn-5	UU	Sn	SnCl ₂	CaCl ₂	Y ₂ O ₃ stabilized MgO
Sn-6	LLNL	Sn	SnCl ₂	LiCl-KCl-CaCl ₂	Y ₂ O ₃ stabilized MgO
Bi-1	BYU	Bi	BiCl ₃	LiCl-KCl-CaCl ₂	Y ₂ O ₃ stabilized MgO

Table 4: Amount of materials used, composition, operating temperature, and duration of each experiment.

Run	Metal (g)	Metal Chloride		Base Salt (g)	Temperature (K)	Duration (hr)
		(g)	(mol%)			
Ce-1	40.55	0	0	43.29	1123	12
Ce-2	43.38	0	0	40.65	1123	12
Ce-3	812.00	100.0	3.35	1300	1123	30
Ce-4	802.2	103.6	3.50	1286	1123	34.6
In-1	12.75	3.012	2.57	57.23	1123	24
Zn-1	20.00	11.6	2.51	219.9	773	24
Sn-1	15.69	---	---	92.50 ¹	1123	12
Sn-2	15.57	---	---	73.79 ¹	1123	3.5
Sn-3	11.14	---	---	60.29 ¹	1123	12
Sn-4	10.93	---	---	61.19 ¹	1123	12
Sn-5	10.49	---	---	60.68 ¹	1123	12
Sn-6	598.7	80.0	1.68	1487.0	673	5
Bi-1	800.0	150.2	2.77	1006.1	683	50

¹The given mass is of the sum of the metal chloride and base salt.

Some exceptions to this general setup are noted in the following subsections, which detail each surrogate system test. The electrorefining conditions are also given, the rationale behind the applied electrorefining voltage/current are given in the results section for each element.

3.1. Cerium

Ce-1 and Ce-2 were performed in an MTI tube furnace (OTF-1200X-S-NT), while Ce-3 and Ce-4 were performed in a custom-built furnace well (309 stainless steel, 163.5 mm Ø x 695.5 mm long) fitted with a custom Thermcraft tube furnace (TSP-8.25-0-15-1C). Before electrorefining was performed, Ce was melted in different types of crucibles (see Table 3) with CaCl₂ to evaluate the extent of the side reactions between Ce, salt, and the crucibles.

After the melt tests had been conducted, Ce electrorefining was performed at a cell voltage of 3 V (see section 4.1). A DC motor (Dayton, 2M168A) and an Asterion 3001 power supply (Ametek

Programmable Power, Inc., AST3001A11B-A000A0A) were used in run Ce-4 to rotate the stir shaft (i.e., anode lead) and provide power to the molten Ce anode and W cathode. The anode lead and cathode ring were made of W (99.95%, Midwest Tungsten).

Scanning electron microscopy (SEM) images were taken using an Apreo Low-Vacuum SEM from ThermoScientific. Samples were transferred from the glovebox to the microscope in sealed plastic containers. It took approximately 30 minutes to transport the sealed plastic containers from the glovebox to the microscopes. After the plastic containers had been opened, the samples were exposed to air for 5-10 minutes at room temperature while they were loaded into the microscope chamber.

3.2. Indium

The In experiments were carried out in a muffle furnace (Thermolyne™ 1300). Cyclic voltammetry (CV) measurements were first performed to characterize the electrochemistry of the system. The working electrode (WE) and counter electrode (CE) were a W rod (2 mm Ø, Alfa Aesar) and a W rod (5 mm Ø, Alfa Aesar) in an In metal pool, respectively. A Ag/AgCl reference electrode (RE) was constructed of a Ag wire immersed in 100% AgCl contained in a MgO tube (Tateho Ozark Technical Ceramics, 99%, 6.35 mm OD, 3.175 mm ID) with a closed end. After these initial electrochemical experiments were performed, an electrorefining experiment was performed. A constant current (-0.08 A) was applied for 24 hrs using a potentiostat (Autolab, PGSTAT302N) (see section 4.2). The WE from the electrochemical experiments served as the cathode for electrorefining while the CE served as the anode. Unlike the general setup, there was no stirring, and a three-electrode setup was used, as the RE was retained during electrorefining to monitor the cathode potential.

Samples were collected for compositional analysis using inductively coupled plasma mass spectroscopy (ICP-MS, Agilent 7900). These samples were collected by immersing a room temperature threaded rod into the molten salt and then quickly removing it. The samples were chipped off from the threaded rod and collected into a pan where the total mass was measured. The samples were dissolved and diluted in 2% HNO₃ and afterward measured with ICP-MS. Scanning electron microscopy with energy-dispersive X-ray spectroscopy (SEM-EDX, Hitachi S-4800 FE-SEM) was also used to characterize the samples.

3.3. Zinc

The Zn experiments were carried out in the same muffle furnace described in Section 3.2. After the initial cyclic voltammogram, an electrorefining experiment using constant current (-0.7 A) was applied for 24 hrs using a potentiostat (Autolab, PGSTAT302N) (see section 4.3). In the CV measurements, the WE and CE consisted of a W rod (99.95%, Midwest Tungsten) and a W ring (99.95%, Midwest Tungsten), respectively. The CE served as the cathode during the electrorefining experiments while the WE served as the anode lead. Again, differing from the general setup, the RE was retained (i.e., three-electrode setup) during electrorefining to monitor the cathode potential. The RE was constructed in the same manner as described in Section 3.2.

Samples for ICP-MS were collected in the same manner as described in Section 3.2. X-ray Diffractometry (XRD, Rigaku Miniflex 600) was also used to characterize the samples.

3.4. Tin

The small-scale Sn experiments were carried out in the same furnace described in Section 3.2. Cyclic voltammograms were collected using a W WE and a Mo CE. A Ag/AgCl RE was fabricated using 1.0-mm diameter Ag wire (Alfa Aesar, 99.99%) enclosed in a mullite ($\text{Al}_6\text{Si}_2\text{O}_3$, McDanel Ceramics) one-end-closed tube. Electrorefining was then conducted using the same cathode and anode lead described in Section 3.2 but with a molten Sn pool in place of the molten In pool. Electrorefining runs were conducted using both constant potential and constant current (see section 4.4). Samples were collected for ICP-MS using the same manner as that described in Section 3.2.

The large-scale Sn experiments were performed in a N_2 atmosphere glovebox with a sealed furnace well with Ar flush (UHP, Praxair), which differs from the general setup described earlier. A Keysight N5700 DC power supply was used to maintain the electrorefining current between 25 and 40 A.

3.5. Bismuth

The same motor, power supply, furnace, and electrodes were used as described for run Ce-4 in Section 3.1. The electrorefining was conducted potentiostatically between 2 and 3.5 V (see Section 4.5). SEM-EDX was conducted using a FEI Helios Nanolab 600 DualBeam FIB/SEM in the same manner as detailed in Section 3.1. The cathode ring samples were sanded with silicon carbide sandpaper with grits between 120 and 3000 before analysis. The samples were milled using the focused ion beam (FIB) capability of the FEI Helios Nanolab 600 DualBeam FIB/SEM.

4. Results

4.1. Cerium

A few melt runs were performed to determine the significance of oxidation of cerium metal by the crucibles. Pictures of the Ce ingots obtained after runs Ce-1, Ce-2, and Ce-3 are shown in Figure 2. The images on the left, middle, and right are respectively from these melt runs in an Al_2O_3 crucible, an yttria-coated Al_2O_3 crucible, and a large-scale MgO crucible. SEM-EDX was conducted on the ingots obtained from Ce-1 and Ce-2 to assess the Ce purity. Figure 3 shows the EDX spectra obtained. Comparing the EDX spectra taken on the surface of the ingots to the spectra taken after the ingots were milled 15 micrometers down using a FIB shows that the O, Mg, Al, Si, and Ti peaks are greatly reduced after milling while the Ce peaks remain the same. Since the EDX spectra of the milled surfaces only have peaks for Ce, the ingots from Ce-1, Ce-2, and Ce-3 are assumed to be high-purity Ce underneath a thin oxide layer.



Figure 2: Ingot recovered from run Ce-1 using an Al_2O_3 crucible (left). Ingot recovered from run Ce-2 using an yttria-coated Al_2O_3 crucible (middle). Ingot recovered from run Ce-3 using a MgO crucible performed at a larger scale (right).

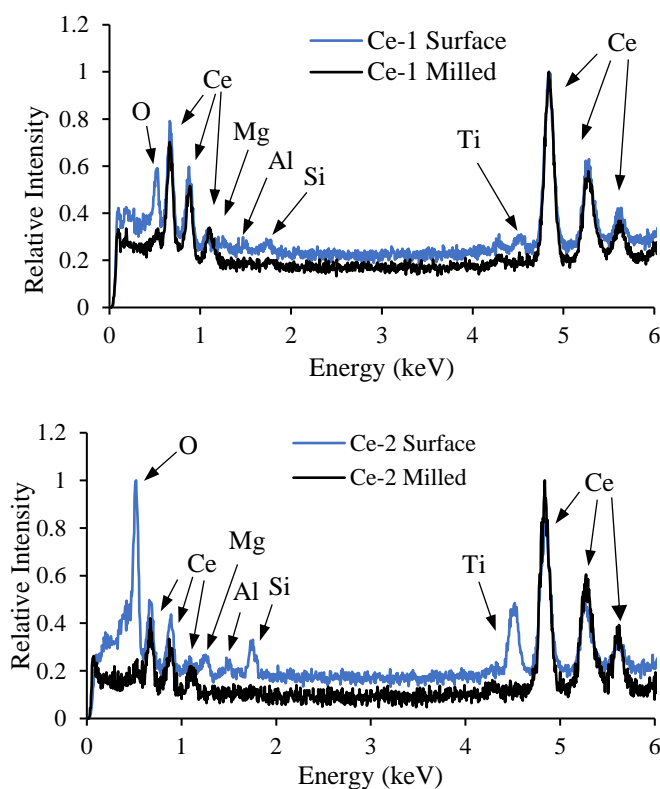


Figure 3: EDX spectra of the ingots from Ce-1 (top) and Ce-2 (bottom).

The initial masses of Ce added for runs Ce-1 to Ce-3 along with the weight of the recovered ingots from each experiment are shown in Table 5. The Ce mass loss was greatest in the yttria-coated Al_2O_3 crucible (Ce-2), but only 1.3% more of the initial mass was lost compared to the Al_2O_3 crucible (Ce-1). The mass loss of the cerium is hypothesized to be due to a reaction occurring between the cerium metal and the crucible to form CeO_2 or some other side product. The rationale for using the yttria coating on the Al_2O_3 crucible was to reduce the reactivity of Ce with the

crucible. The melt experiments conducted did not show the hypothesized reduction to mass loss. While a 5-8% weight loss is not ideal for experiments, it could be accounted for in calculating electrorefining efficiencies and yields. Hence, a large-scale melt experiment (Ce-3) was conducted with a MgO crucible to confirm these results at a different volume-to-surface area ratio (1.2 for Ce-3 vs. 0.36 for Ce-1 & Ce-2), using a different crucible material, and adding CeCl₃ to the salt. The ingot obtained from Ce-3 had a similar appearance to the ingots obtained from Ce-1 and Ce-2, metallic with a thin oxide layer, and it experienced similar Ce mass loss. Given the comparable and manageable mass losses, an electrorefining run using Ce and a MgO crucible without an yttria coating was conducted.

Table 5: Initial and post-melt cerium masses

Run	Initial Mass (g)	Post-melt Mass (g)	Percent Lost
Ce-1	40.548	38.133	5.96%
Ce-2	43.384	40.234	7.26%
Ce-3	812.00	763.28	6.00%

The current profile of run Ce-4 is shown in Figure 4. Initial functionality testing at lower voltages resulted in the lower electrorefining currents, initially, in Figure 4. An electrorefining potential of 1 V corresponded to about 5 A of electrorefining current. 2 V was applied and about 11 A of electrorefining current was observed. After 3 V was applied, the electrorefining current jumped to about 17 A. Due to the current limitations of our power supply (approx. 20 A) the electrorefining potential was held at 3 V for the remainder of the experiment. The current remained between 15-20 Amps for 20 hours. The current then increased before it decreased dramatically at ~30 hours. After a back electromotive force (EMF) measurement, where the cell is allowed to relax for ~1 min and the potential is recorded, the current recovered to previous levels. The decision to terminate the experiment was made after observing the second dramatic decrease in the observed electrorefining current.

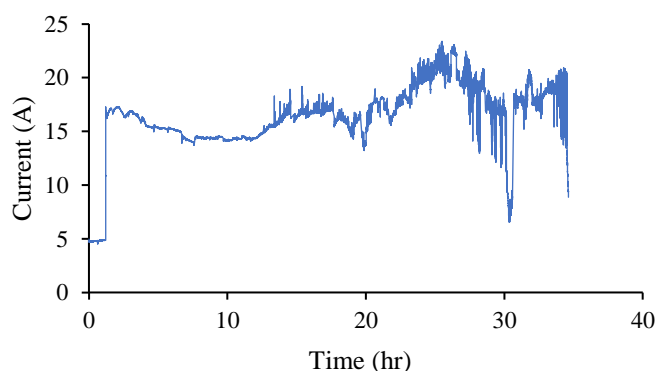


Figure 4: Electrorefining current from experiment Ce-4 in CaCl₂ with 3.50 mol% CeCl₃ added at 1123 K and a cell potential of 3 V after 1.1 hr (Cathode: W ring, Anode lead: W rod in molten Ce).

While there was a measurable electrorefining current for the duration of the experiment, the fluctuations in the current were atypical of an experiment only electrorefining one element. One possible explanation is that Ce was being oxidized throughout the experiment due to side reactions

with electrorefiner components (e.g., crucible, stirrer). The Ce oxidizing could change the surface area of the anode and result in the observed current fluctuations. If Ce oxidation is connected to the current fluctuations, it would explain the gradual onset and subsequent increase in noise, since the extent of Ce oxidation is initially small and increases with time. Another possibility is changing CeCl_3 concentration during electrolysis.

During the electrorefining experiment, Ce-4, no cathode ring was formed, as seen in Figure 5, even though current was passed through the electrorefining cell. However, the recovered anode, also shown in Figure 5, had a mass of 240 grams or 29.6% of the initial weight of Ce added. SEM-EDX analysis was conducted on salt samples from Ce-4 to see if Ce was in different parts of the recovered electrorefining salt. SEM images of salt samples from the Ce-4 run are shown in Figure 6. In the lighter sections seen in each of the SEM images, a high Ce content was detected using EDX. Hence, Ce was unrecoverable and dispersed throughout the salt only when a potential was applied to the cell. While the SEM-EDX analysis conclusively showed the concentration of Ce into a separate phase, it is unable to be directly concluded from this analysis if the Ce is present as a metal, oxide, chloride, or oxychloride as the samples were not able to be prepped for quantitative EDX, specifically.



Figure 5: Bottom view of electrorefining crucible with the base of the outer crucible removed showing that no cathode ring was obtained from run Ce-4 (left); anode leftover from run Ce-4 (right).

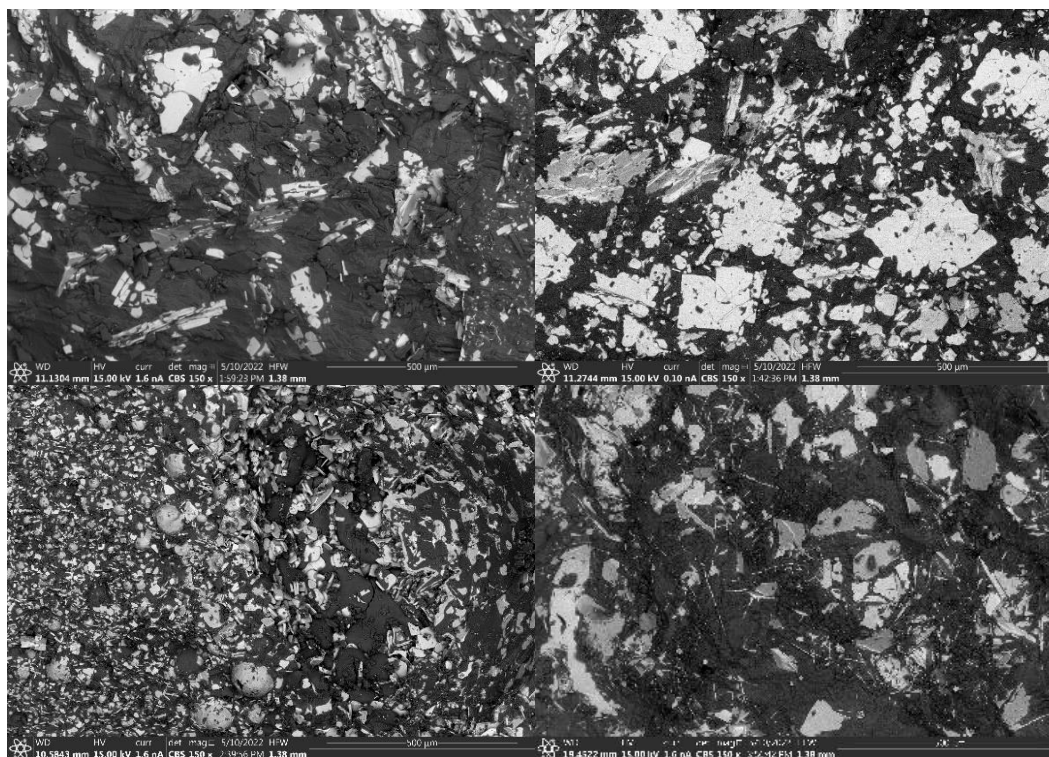


Figure 6: SEM images of salt samples from run Ce-4. Salt above the anode (top left); salt that adhered to Al_2O_3 stirrer (top right); salt below the anode (bottom left); bulk outer crucible salt (bottom right).

4.2. Indium

During the In-1 run, a yellow color vapor was observed after the InCl_3 was added to the CaCl_2 at 1123 K. Table 6 shows the results of the ICP-MS analysis of salt samples before and after the electrorefining experiment. Evidently, most of the InCl_3 volatilized out of the CaCl_2 salt, as enough InCl_3 was added to compose 5 wt.% (2.57 mol%) of the mixture, but only enough InCl_3 remained to compose 0.0124 wt.% (0.0062 mol%) of the salt before electrorefining began. The ICP-MS results show that the salt still had some measurable In content, but most of the added InCl_3 was no longer in the CaCl_2 salt. Sample #3 from the In-1 run shows that the amount of InCl_3 in the salt increased during electrorefining. However, this contradicts with the results from sample #1 and #2 from the same In-1 salt. Sample #3 is likely an erroneous result and could have contained some In metal which would have inflated the In content in the salt.

Table 6: Results of ICP-MS analysis of In content in the salt samples before and after the In-1 run. Concentration is reported in wt.%

Sample	Before Run	After Run
#1	0.012	0.001
#2	0.012	0.003
#3	0.014	0.127
Average	0.0124	0.0436

Before electrorefining, CV was run to identify the potential needed to deposit In metal at the cathode relative to a Ag/AgCl RE. Figure 7 shows the reduction and oxidation peaks for the

$\text{In}^{3+}/\text{In}^+$ and In^+/In couples. The peak assignments are based on a previous publication and alloy phase diagrams [14,15]. $\text{Ca}(\text{In})$ represents calcium-indium alloys generically. There are multiple Ca-In alloys. It is uncertain which alloy(s) are associated with the shoulder at -1.81 V and the oxidation peak at -1.64 V.

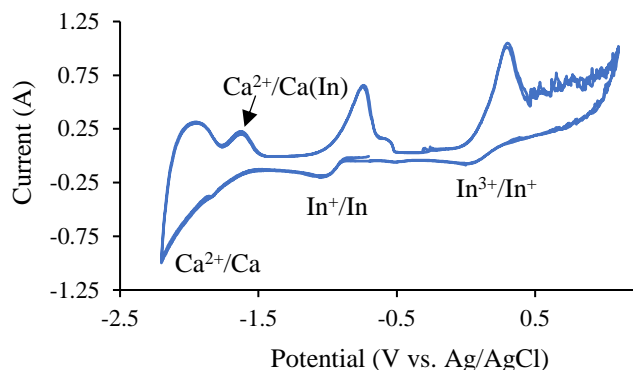


Figure 7: Cyclic voltammogram of $\text{CaCl}_2\text{-InCl}_3$ (0.0062 mol% InCl_3) system at 0.2 V/s and 1123 K (WE: W rod, CE: W rod in molten In, RE: Ag in 100% AgCl).

In In-1, the WE was effectively the cathode by setting the WE current to -0.08 A for 24 hours. The cathode potential is plotted in Figure 8. Figure 9 shows the photos of the salt and crucible after the run. There was some gray, metallic material present between the salt and crucible. To isolate the gray material for analysis, the salt was washed away with water.

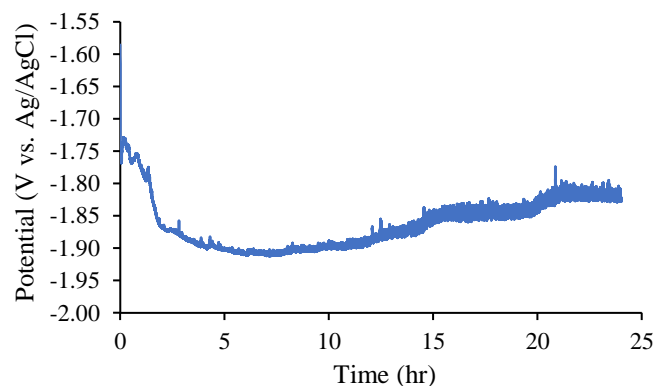


Figure 8: Cathode potential versus time for run In-1 in CaCl_2 at 1123 K at -0.08 A (cathode: W rod, anode: W rod in molten In, RE: Ag in 100% AgCl).

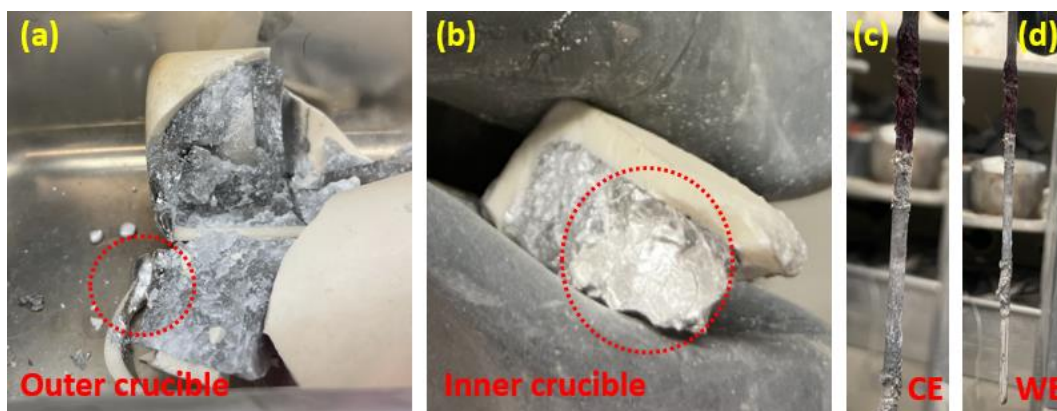


Figure 9: Photos of the salt and indium metal in the bottom of the (a) outer crucible and (b) inner crucible, as well as photos of (c) the anode lead and (d) the cathode after electrodeposition with constant current.

After the salt was dissolved, the gray material was dried in an oven. SEM-EDX was used to identify the compound in three samples of the gray material. A photo of the recovered product is shown in Figure 10. As shown in Table 7, the particles contained on average 95 wt.% In with Mg as the most prevalent minor component.



Figure 10: Photo of cathode deposit from run In-1.

Table 7: SEM-EDX analysis of three points in the cathode product from run In-1. Concentrations reported in wt.%

Sample	#1	#2	#3	Average
In	96.3	91.7	98.2	95.4
Cl	0.6	1.4	---	0.6
Mg	2.1	4.8	1.8	2.9
Ar	1	1	---	0.67
Al	---	0.6	---	0.2
Si	---	0.4	---	0.13

4.3. Zinc

A Zn electrorefining experiment (Zn-1) was run with $\text{CaCl}_2\text{-LiCl-ZnCl}_2$ as the electrolyte. The target ZnCl_2 concentration was 5 wt.%, but, as shown in Table 8, only 2.6 wt.% (1.28 mol%) ZnCl_2 was measured in the salt by ICP-MS. ZnCl_2 is deliquescent and absorbs water, even in inert gas

environments containing trace amounts of moisture [16]. The stock ZnCl_2 likely contained significant moisture, which may have hydrolyzed and formed ZnO [16,17]. The solubility of ZnO in LiCl-CaCl_2 is unknown, but it is likely low (~ 0.01 mol%) based on data in other chloride salts [18,19].

Table 8: ZnCl_2 concentrations measured in salt used for run Zn-1 as measured by ICP-MS.

Sample	ZnCl_2 (wt.%)
#1	2.696
#2	2.846
#3	2.276
Average	2.606

A cyclic voltammogram using a W WE in the $\text{CaCl}_2\text{-LiCl-ZnCl}_2$ salt is shown in Figure 11. The Zn chloride reduction peak was seen at about -0.9 V. Run Zn-1 was run for 24 hr at 773 K with a constant applied current (-0.7 A) and the WE serving as the cathode. The cathode potential versus time for the experiment is plotted in Figure 12. The cathode potential drifted from about -0.9 to -1.35 V over the duration of the experiment.

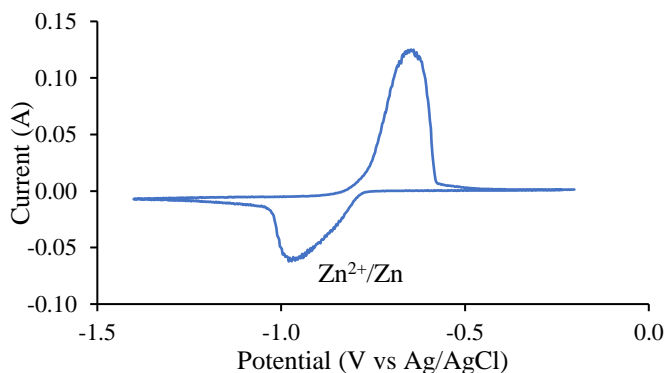


Figure 11: Cyclic voltammogram of $\text{CaCl}_2\text{-LiCl-ZnCl}_2$ (1.28 mol% ZnCl_2) salt prior to run Zn-1 at 773 K (WE: W rod, CE: W rod in molten Zn, RE: Ag in 100% AgCl).

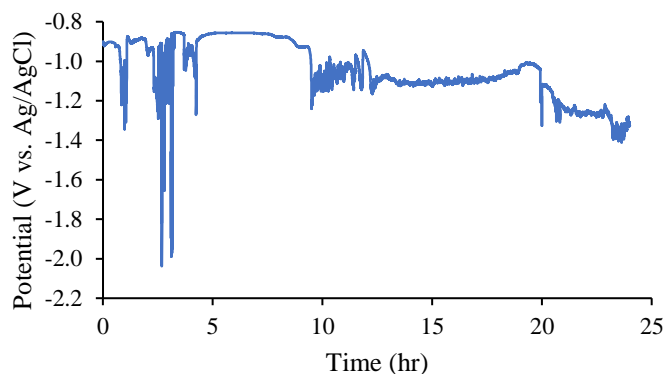


Figure 12: Cathode potential versus time for run Zn-1 in the $\text{CaCl}_2\text{-LiCl}$ eutectic at 773 K and -0.7 A (cathode: W ring, anode lead: W rod in molten Zn, RE: Ag in 100% AgCl).

After the run had cooled, the crucible was removed and broken open to collect any product that had formed. Figure 13 shows images of the bottom of the crucible after run Zn-1 and of the metal powder recovered from the outer crucible. The mass of metal powder collected was 2.0 g. XRD was performed on the powder shown in Figure 13(b) and is shown in Figure 14. The XRD spectrum showed that the metal powder collected was a combination of Zn, ZnO, LiCl, and CaCl₂, confirming that Zn metal was collected in the outer crucible.

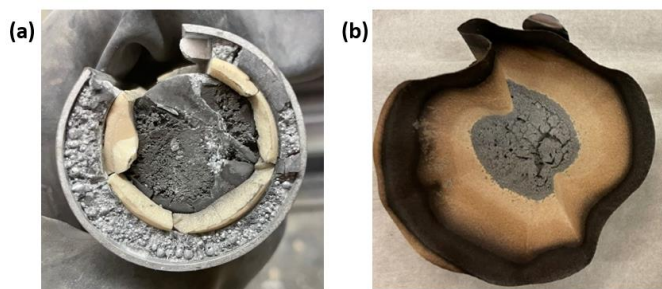


Figure 13: Photographs of the (a) the crucible with bottom broken off after run Zn-1 and (b) metal powder recovered from the outer crucible and rinsed to remove salt.

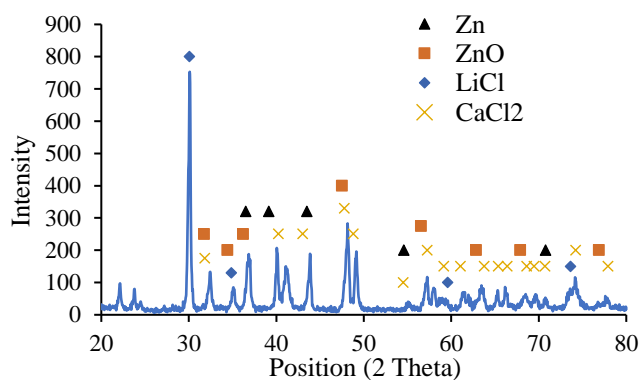


Figure 14: XRD of metal powder collected from the bottom of the outer crucible after run Zn-1. Black triangles indicate the presence of Zn metal.

4.4. Tin

A yellow vapor was observed after initially adding SnCl₂ (5 wt.% targeted) to CaCl₂ that persisted for approximately 1.5 hr. ICP-MS analysis of three salt samples indicated an average of only 0.0062 wt.% (0.0036 mol%) SnCl₂. Therefore, there was 99.9% volatilization of the SnCl₂ from CaCl₂ at 1123 K. This salt was used in electrorefining run Sn-1 using a controlled cathode potential of -0.6 V but resulted in no current and no evidence of Sn deposition in the outer crucible. For the Sn-2 run, enough SnCl₂ was added to result in a measured SnCl₂ concentration of 0.16 wt.% (0.094 mol%). Table 9 gives the ICP-MS results for salt samples taken prior to each of the five Sn electrorefining runs that were performed at small-scale.

Table 9: Results of ICP-MS analysis of samples before Sn electrorefining runs Sn-1 through Sn-5 in CaCl_2 .

Run	SnCl_2 concentration (wt.%)			
	1	2	3	Average
Sn-1	0.0075	0.0057	0.0055	0.0062
Sn-2	0.157	0.173	0.163	0.164
Sn-3	0.077	0.075	0.075	0.075
Sn-4	0.059	0.050	0.051	0.053
Sn-5	0.025	0.020	0.015	0.020

CV was performed in the CaCl_2 - SnCl_2 salt mixtures using a W WE, a Mo CE, and a Ag/AgCl RE. Figure 15 shows the plot of the cyclic voltammogram recorded in the run Sn-2 salt. A reduction peak appeared at about -0.3 V vs. Ag/AgCl. This is in the vicinity of the standard reduction potential for SnCl_2 at 1123 K (-0.3285 V) and thus assumed to indicate the presence of SnCl_2 dissolved in the salt. The standard potential was calculated using the ΔG of formation for SnCl_2 and AgCl at 1123 K. As the boiling point of SnCl_2 is less than 850 °C, the ΔG of formation for SnCl_2 in the gas phase was used [7].

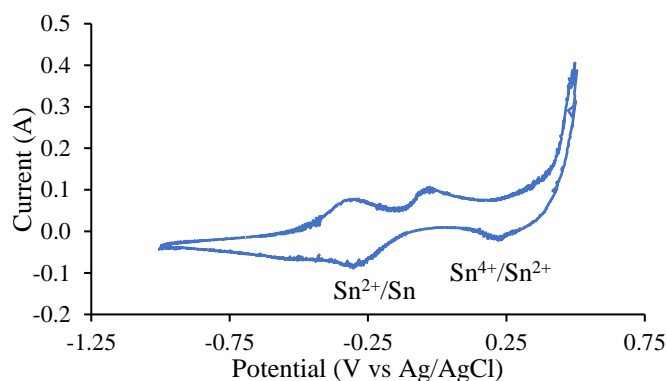


Figure 15: Cyclic voltammogram of CaCl_2 - SnCl_2 (0.094 mol% SnCl_2) system at 0.2 V/s and 1123 K prior to run Sn-2 (WE: W rod, CE: Mo rod, RE: Ag in 100% AgCl).

Runs Sn-2 and Sn-3 were performed at constant current (-0.04 A). A W rod partially immersed in Sn metal was used as the anode lead. The cathode potentials for these two runs are shown in Figure 16. The cathode potential initially dropped to -1.6 V in Sn-2 and -1.9 V in Sn-3 and then increased gradually over the span of both runs. These potentials are much lower than the SnCl_2 reduction potential shown in Figure 15 but still higher than the reduction potential of CaCl_2 (approx. -2 V vs. Ag/AgCl) [20]. However, this does not preclude the possibility of Sn-Ca alloy forming and causing the potentials observed in Figure 16 [15].

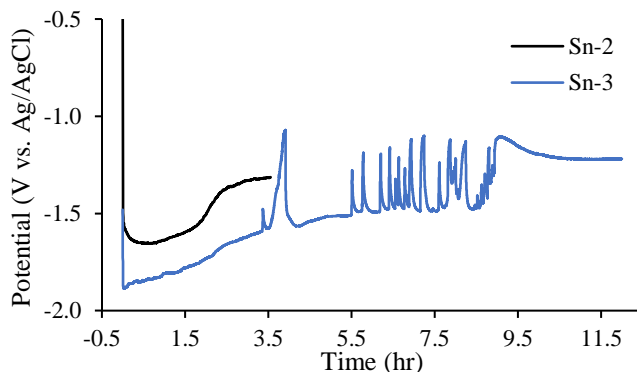


Figure 16: Cathode potential versus time in runs Sn-2 and Sn-3 in CaCl_2 at 1123 K. Both runs were held at a constant current of -0.04 A (cathode: W rod, anode lead: W rod in Sn metal, RE: Ag wire in 100% AgCl).

There was no appreciable cathode product collected in any of the small-scale Sn runs in CaCl_2 . Anode mass measurements for runs Sn-1 through Sn-5 are shown in Table 10. Cell efficiencies were calculated based on the actual anode mass loss divided by the amount predicted based on the total charge transferred during each run. There was a large variation in cell efficiency for the four runs—44 to 95%. It was not possible to isolate the cathode deposit to measure its mass and calculate a mass balance.

Table 10: Mass change for Sn metal anode for Sn electrorefining runs

Run	Mode	Charge (C)	Sn metal in anode (g)			Anodic Efficiency (%)
			Before	After	loss	
Sn-1	Potentiostatic (-0.6 V)	---	15.6913	15.5658	0.1255	---
Sn-2	Galvanostatic (-0.04 A)	504	15.5652	15.2657	0.2995	95
Sn-3	Galvanostatic (-0.04 A)	1728	11.1353	10.6719	0.4634	44
Sn-4	Galvanostatic (-0.02/-0.03 A)	1152	10.9272	10.4558	0.4714	68
Sn-5	Galvanostatic (-0.04 A)	>576*	10.4867	9.7877	0.699	---

*estimated, potentiostat software failed to save data

The large-scale Sn electrorefining experiment (Sn-6) took place in LiCl-KCl-CaCl_2 with 5.1 wt.% SnCl_2 weighed out and added. Electrorefining was performed under controlled current stepped from 25 to 40 A. 598.7 g of Sn metal was placed in the inner MgO crucible. After 5 hours of electrorefining 281.0 g of Sn was left in the inner MgO crucible, and 302.5 g of Sn was recovered in one piece in the outer crucible, while the balance of Sn was held up on the stirrer. The cathode current efficiency was estimated at 90%. Figure 17 shows a photo of the anode heel and the cathode product.

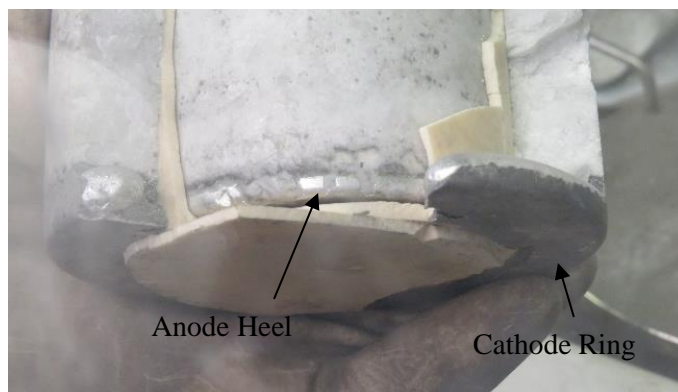


Figure 17: Picture of cathode ring and anode heel obtained from Sn-6.

4.5. Bismuth

The electrorefining voltage applied across the electrorefining cell during Bi-1 is shown in Figure 18. Initially 2.0 V was applied to test the cell, after which, 3.5 V was applied for ~5 hours. Back EMF measurements were taken every 1-2 hours. A back EMF of 2 V was seen after applying 3.5 V which could be indicative of Ca co-depositing with Bi. The voltage was lowered to 2 V to ensure that Ca was not co-depositing with Bi. A back EMF of 2 V was not seen after lowering the electrorefining voltage to 2 V. The back EMF recorded during Bi-1 is shown in Figure 19.

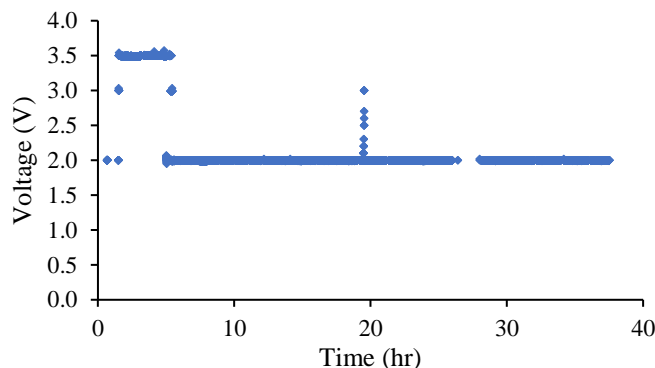


Figure 18: Electrorefining voltage versus time during run Bi-1 in LiCl-KCl-CaCl_2 at 683 K with 2.77 mol% BiCl_3 added (cathode: W ring, anode lid: W stir shaft in Bi metal).

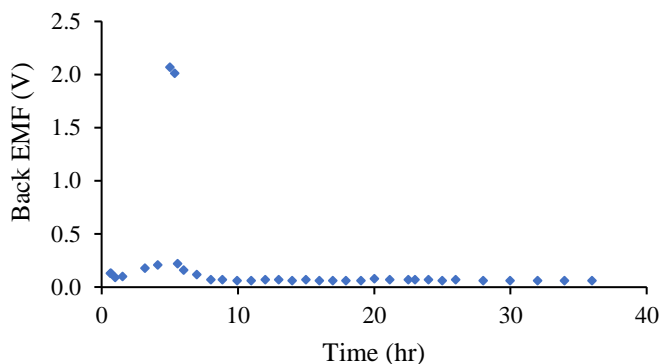


Figure 19: Back EMF voltage versus time during run Bi-1 in LiCl-KCl-CaCl_2 at 683 K with 2.77 mol% BiCl_3 added (cathode: W ring, anode lid: W stir shaft in Bi metal).

The current recorded during Bi-1 is shown in Figure 20. When the voltage applied was 3-3.5 V (~1.5-5 hours), the current fluctuated between 3 and 13 A, which is atypical of electrorefining. After the electrorefining voltage was changed to 2 V, the current held steady at approximately 5 A for 15 hours. At that time, it was discovered that a loose connector had decreased the current going through the electrorefining cell. Once the connector was tightened, the current increased to approximately 7 A and held steady there for approximately 20 hours. The gap in data in Figure 20 between hour 26.4 and hour 28 was due to a computer malfunction. It was assumed in the efficiency calculations that the current remained at 7 A during that gap. The run was terminated after approx. 50 hours however, the laptop also stopped recording data approximately 13 hours before the run was terminated. A current of 6.9 A was assumed for the remainder of the run as that was the last current measurement recorded. This enabled a conservative estimate of the coulombic efficiency to be made for the electrorefining run.

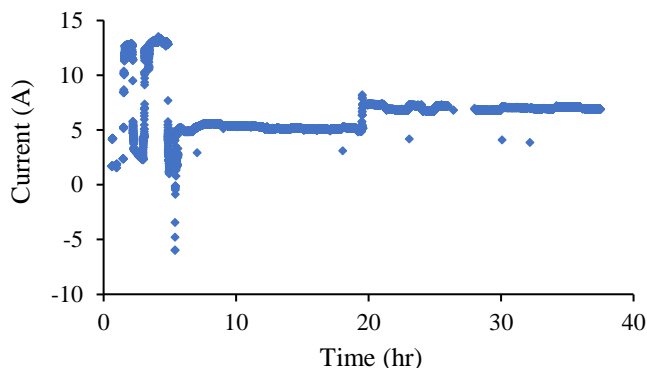


Figure 20: Electrorefining current versus time measured during run Bi-1 in the LiCl-KCl-CaCl_2 eutectic at 683 K with 2.77 mol% BiCl_3 added (cathode: W ring, anode lead: W rod in molten Bi).

Pictures of the Bi cathode ring and anode from run Bi-1 are shown in Figure 21. 663.5 grams of the 800 grams of Bi initially added was recovered as the cathode ring. The recovered anode

weighed 69.6 grams. ICP-MS results conducted on samples from the cathode ring are shown in Table 11. SEM-EDX was also conducted on the cathode ring. The obtained spectra are shown in Figure 21. The only significant peaks after the sample had been milled approximately 10 μm were Bi peaks. The O peak was indecipherable after the sample had been milled, which indicated that O was only a surface impurity introduced by the sample having contacted the crucible or being exposed to air when the sample was transferred into the FIB-SEM. The results of ICP-MS and EDX analysis showed that there were no major impurities in the bulk of the cathode ring. A Ga peak did appear but that was from the milling process used.

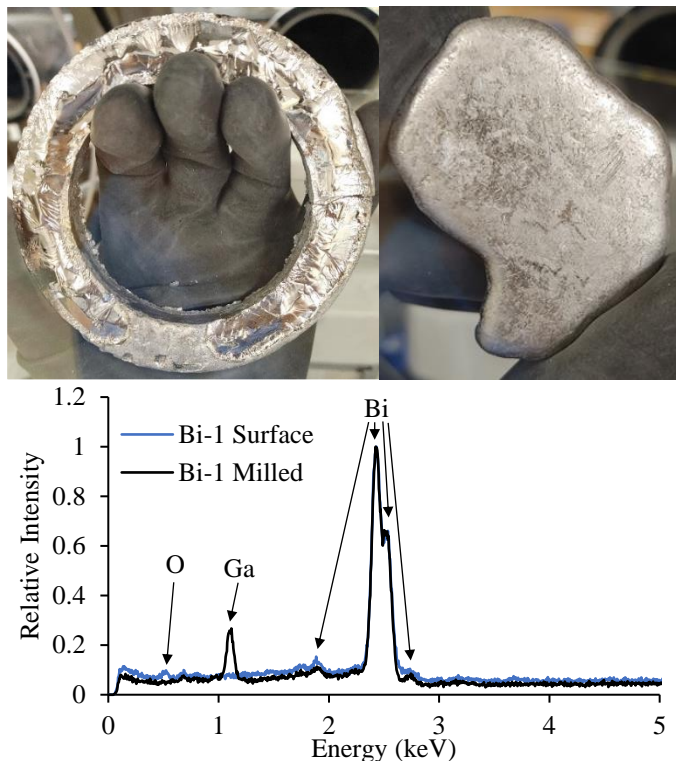


Figure 21: Cathode ring (top left), anode heel (top right), and EDX spectra of sample from cathode ring (bottom) from experiment Bi-1.

Table 11: Bi concentrations measured in cathode ring recovered from run Bi-1 as measured by ICP-MS.

Sample	Bi (wt.%)
#1	96.582
#2	102.371
#3	99.571
Average	99.508

5. Discussion

5.1. Cerium

While Ce is the most chemically like plutonium, the electrorefining experiment conducted showed that Ce cannot be successfully electrorefined to form a cathode ring using common electrorefining materials (i.e., MgO crucible, CaCl_2). The lack of systemic similarity (i.e., no cathode ring), makes

Ce an unsuitable surrogate for plutonium electrorefining. Originally, the lack of a cathode ring was hypothesized to be due to oxidation of the Ce metal by the ceramic crucibles. However, the melt tests demonstrated that this only leads to minimal (5-7%/day) losses. When applying a current to the cell and stirring the anode, the Ce was transported out of the anode into the molten salt. For the cell to operate, reduction had to occur at the cathode, but it did not yield a coalesced Ce product. Rather, the Ce remained dispersed throughout the salt.

Based on the SEM images in Figure 6 and previous research, it is confirmed in this work that Ce does not coalesce in molten CaCl_2 but forms a colloid mixture with regions richer in Ce. Mishra et al. observed this colloid mixture in their work as well, reporting that both “cerium and bismuth do not separate from the $[\text{CaCl}_2]$ salt as they form a colloid suspension” [21]. They also observed “a black salt layer consisting of cerium metal, gallium, cerium oxy-chloride and calcium chloride” [22]. Their chemical analysis revealed that the black salt, also observed in this study, contained 79 wt.% Ce. These observations agree with our work, with the exception of Bi forming a colloid mixture. The key difference is that Mishra et al. used pure CaCl_2 while a eutectic salt mixture was used in our Bi electrorefining runs.

While this work only tested one set of electrorefining conditions (potentiostatic at 3 V), previous work by Raraz attempted both potentiostatic and galvanostatic electrorefining with similar results [12]. Raraz reported potentiostatic electrorefining at 4.6 V and galvanostatic electrorefining at a current density of 0.19 A/cm^2 (1.2 A/in^2) in one test and currents from 0.9-1 A in other tests. A more recent work had similar challenges getting Ce to coalesce in molten KCl using galvanostatic electrorefining at 4.0 A [23]. This same work saw some success using chlorine generation in-situ to help the Ce to successfully coalesce. Thus, the conditions of applying power to the electrorefining cell appear to have little effect on coalescence of Ce. Rather, an additive that promotes the coalescence of Ce metal may be a more probable path for being able to successfully electrorefine Ce in molten CaCl_2 .

5.2. Indium

Indium can be electrorefined in CaCl_2 , but the InCl_3 concentration in the salt is extremely low. While In has most of the requisite properties to be a good surrogate for plutonium electrorefining, the boiling point of InCl_3 is below the operating temperature of 1123 K. ICP-MS analysis showed that the InCl_3 added to the CaCl_2 did not remain in solution. 5 wt.% InCl_3 was targeted, but less than 0.1 wt.% remained in the melted salt. This loss of InCl_3 in the molten salt solution was likely enhanced by the reduction of InCl_3 to InCl which would proceed naturally in the presence of In metal (i.e., $\text{InCl}_3 + 2\text{In} \leftrightarrow 3\text{InCl}$, $\Delta G^\circ(1123 \text{ K}) = -136 \text{ kJ/mol}$) [7]. The boiling point of InCl (811 K) being even less than that of InCl_3 .

Indium ions were successfully reduced from the molten salt to In metal despite its low concentration. The recovered metal was shown to be mostly In with some Mg impurities using SEM-EDX. The Mg impurities could be due to co-reduction of Mg impurities in the stock salt or leached from the crucible during the InCl_3 reduction. Significantly negative potentials were observed (-1.9 V vs. Ag/AgCl , see Figure 8) during In electrorefining making Mg reduction ($E^\circ \approx -1.63 \text{ V vs. Ag/AgCl}$ at 1123 K [7]) a possibility. The reduction of Mg has been observed at ~ 0.3

V vs. Ca^{2+}/Ca at 1123 K in CaCl_2 [24]. The Ca^{2+}/Ca equilibrium potential is estimated to be -2.1 V vs. Ag/AgCl from Figure 7, which makes -1.9 V vs. Ag/AgCl a reasonable potential for Mg deposition.

While In could be successfully deposited out of a CaCl_2 solution at the plutonium electrorefining conditions, InCl_3 is unable to stay in the molten CaCl_2 salt at a sufficient concentration to support electrorefining at an appreciable rate. Hence, In is an unattractive surrogate in molten CaCl_2 for plutonium electrorefining due to the slow mass transfer rates that would result from a very low In ion concentration. In could potentially be used in one of the eutectic salts, but the formation of InCl is expected to still occur limiting In electrorefining to below the boiling point of InCl (811 K).

5.3. Zinc

When using $\text{CaCl}_2\text{-LiCl}$ as the electrolyte and running at 773 K, Zn appears to be an adequate surrogate for plutonium. Compared to In and Sn, higher concentration of the soluble salt can be attained in this system. Zn metal was collected in the outer crucible and identified using XRD. While Zn was recovered, there was not a coalesced product and the salt had to be rinsed off to separate the Zn after the experiment, which will complicate experiments and the analysis of the product.

5.4. Tin

Sn was deposited out of a $\text{SnCl}_2\text{-CaCl}_2$ molten salt in trace quantities. Similar issues were experienced as those of In where the SnCl_2 did not appreciably stay in solution at 1123 K. However, Sn was successfully electrorefined at a large-scale in LiCl-KCl-CaCl_2 eutectic at 673 K. Thus, chemical similarity to plutonium electrorefining was sacrificed, but the electrorefining configuration (i.e., molten metal on bottom with molten salt on top) was maintained. Despite the short duration of electrorefining, a cathode ring was obtained with 50.5% yield and 90% current efficiency.

SnCl_2 (boiling point: 896 K) is less volatile than BiCl_3 (boiling point: 720 K) and Sn can be alloyed with Cu for further research of electrorefining with impurities in the anode. However, Sn is lighter than Bi which can result in less stability at the anode/electrolyte interface when mixing and slower coalescences into a ring. For example, the furnace needed to stay heated after run Sn-6 for a couple hours so that the cathode ring could be formed. The slower coalescences may be less of an issue in longer electrorefining runs.

A potential challenge for Sn as a surrogate is the multiple stable cations (Sn^{2+} , Sn^{4+}). This could lead to a circular process of Sn^{2+} being oxidized to Sn^{4+} at the anode, then Sn^{4+} being reduced to Sn^{2+} . When using Sn as a surrogate, careful control or monitoring of the cell potential is needed to prevent this circular process from significantly impacting electrorefining efficiency.

5.5. Bismuth

While using Bi as a surrogate for plutonium electrorefining sacrifices chemical similarity, the physical configuration of electrorefining Bi is similar to plutonium electrorefining. Bi was able to

be oxidized from the inner molten metal anode, transported through the molten salt electrolyte to the cathode where it was reduced and collected in the outer annulus under the molten salt. The signal trends (i.e., current, or potential) are qualitatively the same as plutonium electrorefining. A cathode ring was obtained with 77% yield and 83% coulombic efficiency at the cathode.

6. Conclusions

A surrogate to simulate plutonium electrorefining would reduce the cost and complexity of studying processes occurring during electrorefining and experimenting with the electrochemical parameters. However, no surrogate was found that is chemically similar and maintains the same electrorefining configuration. The required boiling point, melting point, density, and electrochemical standard potential for metal surrogates and their corresponding chloride salts for electrorefining in molten CaCl_2 resulted in only three potential surrogates: Ce-CeCl₃, In-InCl₃ and Pb-PbCl₂. Using molten LiCl-KCl-CaCl₂ eutectic salt sacrificed chemical similarity but lowered the operating temperature of the electrorefiner. This change increased the pool of potential surrogates from three to seven with the addition of Bi-BiCl₃, Sn-SnCl₂, Zn-ZnCl₂, and Tl-TlCl. Pb and Tl were eliminated from this study due to their toxicity.

All the potential surrogates tested in molten CaCl_2 at 1123 K were unable to be successfully electrorefined. While Ce was identified as an ideal surrogate based on its properties, its tendency to remain intimately mixed with CaCl_2 meant that no cathode ring was produced from the Ce electrorefining experiments conducted as a part of this study. InCl₃ could not remain in the molten CaCl_2 salt to support an appreciable current. Zn showed a small amount of success in being electrorefined at a lower temperature in LiCl-CaCl₂. However, the Zn product did not coalesce into an easily separable form and needed to be rinsed with water to separate it from the salt. Bi and Sn were able to be successfully electrorefined using a similar configuration (i.e., molten salt above molten metal) to plutonium electrorefining, but a eutectic molten salt composed of LiCl-KCl-CaCl₂ was used with an operating temperature of 773 K or lower. Bi and Sn both coalesced into an easily separable product ring. While the change in salt and operating temperature sacrifices most of the chemical similarities to plutonium electrorefining, there is still value in identifying other elements that can simulate the molten-metal, molten-salt dynamics of plutonium electrorefining. These surrogates can potentially be used to investigate fundamental aspects, such as charge transfer and mass transport, of electrorefining a dense molten metal in molten salts. In future work, impurities will be introduced to the Bi and/or Sn metal feed (i.e., anode) to further investigate their suitability as plutonium electrorefining surrogates and the effect of different applied waveforms on electrorefining performance.

Acknowledgements

This work was performed under the auspices of the U.S. Department of Energy by Lawrence Livermore National Laboratory under Contract DE-AC52-07NA27344.

We also acknowledge and thank Mario Gonzalez for his aid in analyzing the XRD data for the zinc product.

References

- [1] T. Paget, J.A. McNeese, K. Fife, M. Jackson, R. Watson, Chapter 6. Molten Salt Chemistry of Plutonium, in: D.L. Clark (Ed.), *Plutonium Handb.*, 2nd ed., American Nuclear Society, La Grange Park, IL, 2019.
- [2] J.L. Willit, W.E. Miller, J.E. Battles, Electrorefining of uranium and plutonium — A literature review, *J. Nucl. Mater.* 195 (1992) 229–249. [https://doi.org/10.1016/0022-3115\(92\)90515-M](https://doi.org/10.1016/0022-3115(92)90515-M).
- [3] J.L. Long, R.D. Schweikhardt, *Plutonium Electrorefining at Rocky Flats*, Dow Chemical Co., Rocky Flats Div., Golden, CO, 1967. <https://doi.org/10.2172/4434340>.
- [4] L.J. Mullins, A.N. Morgan, *Review of operating experience at the Los Alamos Plutonium Electrorefining Facility, 1963-1977*, Los Alamos National Lab., NM (USA), 1981. <https://doi.org/10.2172/5555056>.
- [5] International Atomic Energy Agency, *IAEA safeguards glossary: 2001 edition*, International Atomic Energy Agency, Vienna, 2002. https://www.iaea.org/sites/default/files/iaea_safeguards_glossary.pdf (accessed July 12, 2021).
- [6] U.S. Nuclear Regulatory Commission, *10 CFR Part 74: Material Control and Accounting of Special Nuclear Material*, 2011. <https://www.govinfo.gov/app/details/CFR-2011-title10-vol2/CFR-2011-title10-vol2-part74>.
- [7] I. Barin, *Thermochemical Data of Pure Substances*, 3rd ed., VCH Verlagsgesellschaft mbH., Weinheim, 1995.
- [8] R.O. Hoover, D. Yoon, S. Phongikaroon, Effects of temperature, concentration, and uranium chloride mixture on zirconium electrochemical studies in LiCl-KCl eutectic salt, *J. Nucl. Mater.* 476 (2016) 179–187. <https://doi.org/10.1016/j.jnucmat.2016.04.037>.
- [9] K. Yasuda, T. Nohira, Y.H. Ogata, Y. Ito, Electrochemical window of molten LiCl–KCl–CaCl₂ and the Ag+/Ag reference electrode, *Electrochimica Acta.* 51 (2005) 561–565. <https://doi.org/10.1016/j.electacta.2005.05.014>.
- [10] E.R. Van Artsdalen, I.S. Yaffe, Electrical conductance and density of molten salt systems: KCl–LiCl, KCl–NaCl and KCl–KI, *J. Phys. Chem.* 59 (1955) 118–127. <https://doi.org/10.1021/j150524a007>.
- [11] G.J. Janz, R.P.T. Tomkins, C.B. Allen, J.R. Downey, G.L. Garner, U. Krebs, S.K. Singer, *Molten salts: Volume 4, part 2, chlorides and mixtures—electrical conductance, density, viscosity, and surface tension data*, *J. Phys. Chem. Ref. Data.* 4 (1975) 871–1178. <https://doi.org/10.1063/1.555527>.
- [12] A.G. Raraz, *Optimization of Plutonium Electrorefining Through Modeling and Model Materials*, Ph.D., Colorado School of Mines, 1994. <https://www.proquest.com/docview/2221128728/citation/17763D8B10F14265PQ/1> (accessed February 9, 2021).
- [13] V. Dimitrov, K. Kostova, M. Genov, Anhydrous cerium(III) chloride — Effect of the drying process on activity and efficiency, *Tetrahedron Lett.* 37 (1996) 6787–6790. [https://doi.org/10.1016/S0040-4039\(96\)01479-7](https://doi.org/10.1016/S0040-4039(96)01479-7).
- [14] M. Mohamedi, S. Martinet, J. Bouteillon, J.C. Poignet, Comprehensive examination of the electrochemistry of indium in the molten LiCl–KCl eutectic, *Electrochimica Acta.* 44 (1998) 797–803. [https://doi.org/10.1016/S0013-4686\(98\)00239-4](https://doi.org/10.1016/S0013-4686(98)00239-4).
- [15] H. Okamoto, M.E. Schlesinger, E.M. Mueller, *ASM Handbook: Alloy Phase Diagrams*, ASM International, Metals Park, OH, 2016.

- [16] R.F. Watson, G.S. Perry, Solubility of ZnO and hydrolysis of ZnCl₂ in KCl melts, *J. Chem. Soc. Faraday Trans.* 87 (1991) 2955–2960. <https://doi.org/10.1039/FT9918702955>.
- [17] S. Niazi, E. Olsen, H.S. Nygård, Hydrolysis of eutectic compositions in the ZnCl₂:KCl:NaCl ternary system and effect of adding ZnO, *J. Mol. Liq.* 317 (2020) 114069. <https://doi.org/10.1016/j.molliq.2020.114069>.
- [18] V.L. Cherginets, On studies of oxide solubilities in melts based on alkaline halides, *Electrochimica Acta.* 42 (1997) 3619–3627. [https://doi.org/10.1016/S0013-4686\(97\)00031-5](https://doi.org/10.1016/S0013-4686(97)00031-5).
- [19] V.L. Cherginets, E.G. Khailova, On the solubilities of bivalent metal oxides in molten alkaline chlorides, *Electrochimica Acta.* 39 (1994) 823–829. [https://doi.org/10.1016/0013-4686\(94\)80031-6](https://doi.org/10.1016/0013-4686(94)80031-6).
- [20] M. Schvaneveldt, R. Fuller, D. Rappleye, Electroanalytical measurements of lanthanum (III) chloride in molten calcium chloride and molten calcium chloride and lithium chloride, *J. Electroanal. Chem.* 918 (2022) 116442. <https://doi.org/10.1016/j.jelechem.2022.116442>.
- [21] B. Mishra, D.L. Olson, W.A. Averill, Application of Molten Salts in Pyrochemical Processing of Reactive Metals, *ECS Proc. Vol. 1992–16* (1992) 184. <https://doi.org/10.1149/199216.0184PV>.
- [22] B. Mishra, J.J. Moore, A.M. Murray, Pyrochemical Processing of Molten Salt for Actinide Recovery, in: *Proc. Int. Symp. Molten Salt Chem. Technol. 1993*, Electrochemical Society, Incorporated, Honolulu, HI, 1993: pp. 210–219.
- [23] Z. Tian, Y. Zhong, Z. Wang, M. Qin, X. Li, S. Meng, Y. Chen, J. Liu, Y. Zhu, K. Du, H. Yin, D. Wang, Study on Aggregation Forming of Cathode Liquid Cerium Metal in Molten Salt Electrorefining Process, in: C. Liu (Ed.), *Proc. 23rd Pac. Basin Nucl. Conf. Vol. 3*, Springer Nature, Singapore, 2023: pp. 920–931. https://doi.org/10.1007/978-981-19-8899-8_88.
- [24] A.M. Martínez, B. Børresen, G.M. Haarberg, Y. Castrillejo, R. Tunold, Electrodeposition of Magnesium from CaCl₂ - NaCl - KCl - MgCl₂ Melts, *J. Electrochem. Soc.* 151 (2004) C508. <https://doi.org/10.1149/1.1758814>.